PCCP

Accepted Manuscript

ROYAL SOCIETY OF CHEMISTRY

www.rsc.org/pccp

By contrasting for the first time the non-relativistic and relativistic characterization of the electronic states of iodocarbyne, we provide a very reliable description of this species that we expect can motivate and guide the spectroscopist in its experimental investigation.

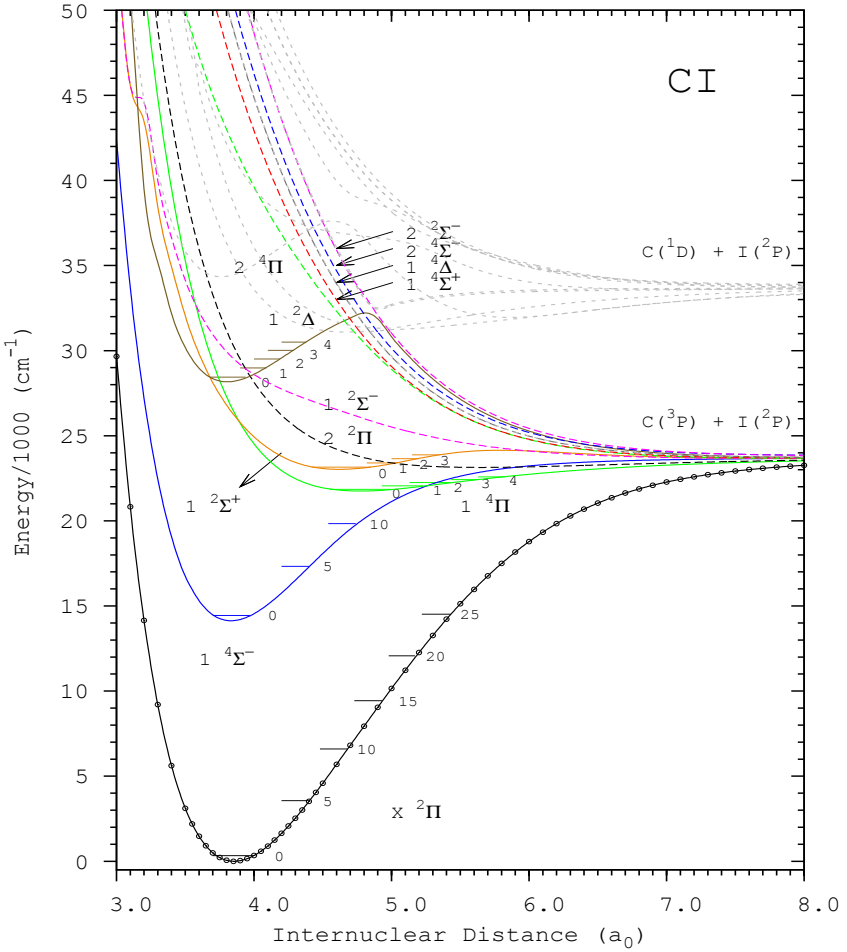

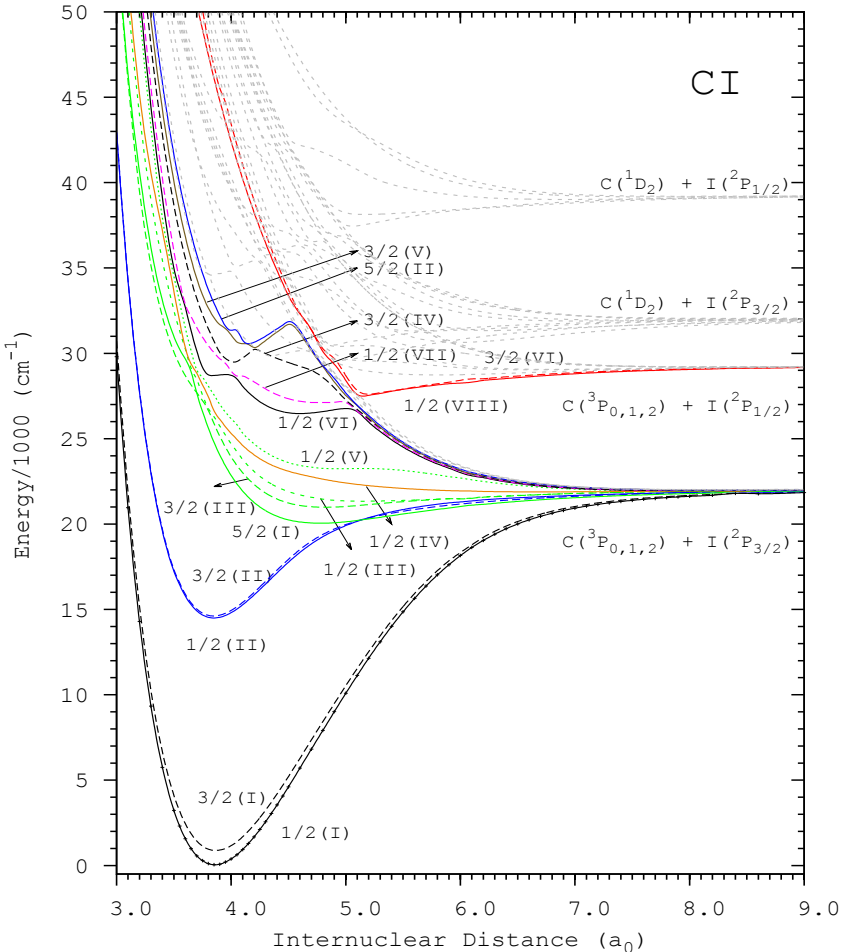

Revised article submitted to Physical Chemistry Chemical Physics, March 11

Exploring the electronic states of iodocarbyne: a theoretical contribution

Tiago Vinicius Alves and Fernando R. Ornellas*

Departamento de Química Fundamental, Instituto de Química,
Universidade de São Paulo, Av. Prof. Lineu Prestes, 748,
São Paulo, São Paulo, 05508-000, Brazil

*Fax: +55 11 3815 5579
Email address: frornell@usp.br

Abstract

A manifold of electronic states correlating with the two lowest-lying dissociation channels of the species iodocarbyne (CI) is theoretically characterized for the first time in the literature. A contrast between the Λ + S and the relativistic (Ω) descriptions clearly shows the effect of perturbations on electronic states above 20 000 cm^{-1} and the potential difficulties to de

tect them experimentally. For the bound states, spectroscopic parameters were evaluated, as well as the dipole moment functions. Similarly to CO, the polarity predicted for this iodocarbyne is $C^{\delta-}I^{\delta+}$; as illustrated in the text, this is also the case for the other halocarbynes. As a potential mechanism for the experimental spectroscopic characterization of CI, we suggest the radiative association between C and I atoms, with light emitted in the red region of the visible spectra. Transitions probabilities were also evaluated predicting very weak intensities. For the states 1/2(II) and 3/2(II), we have estimated radiative lifetimes of 7.1 and 714 m*s*, respectively.

1. Introduction

Carbenes and carbynes form special classes of short lived reactive intermediates where the carbon atom shows a divalent and a monovalent nature, respectively. In carbenes, the two unpaired electrons can couple either as singlet or triplet states very close in energy making the spectroscopy of this singlet-triplet splitting, as well as their reactivity, the subject of extensive investigations in the literature. [1-3] Whereas a large number of studies have been reported for carbenes, this is not the case for carbynes.[4] The carbon atom, monovalently bonded to a ligand, has three remaining electrons that can give rise to either doublet or quartet states. This electron-rich carbon center makes the carbynes very reactive species. The simplest prototype of a carbyne is the CH radical, but carbynes have been known for a long time to bind as trivalent ligands to transition metal complexes.[5,6] The role of ruthenium carbyne complexes as catalysts for olefin methatesis, for example, is discussed by Shao *et al*.,[7] and the syntheses, structures and reactivity of heavier analogues of transition metals is the subject of a short review by Wu.[8]

Halocarbynes or halomethylidynes have been generated by flash and laser photolysis of haloderivatives of C_1 and C_2 hydrocarbons. In the gas phase, studies of the reaction of CF, CCl, and CBr with alkenes were carried out by Ruzsicska *et al*., in which kinetic absorption spectroscopy was used to monitor the concentration of the carbyne species.[9] Of the halocarbynes, iodocarbyne (CI) is the species least investigated experimentally. The ion-molecule collision of I^- ions with CO, with the detection of O^- is an experimental fact from which the existence of CI has been inferred.[10] The potential presence and role that CI could play in atmospheric and combustion studies is still unknown. In the case of CBr, for example, it is known to be a dissociation product of bromoform,[11] and as a bromine-containing radical it can also participate in the destruction of ozone.[12] The knowledge of its electronic states and allowed transitions, as carried out by Burrill and Grein[13] for CBr, is thus very important to clarify experimental results

that can help one monitor its concentration by spectroscopic techniques. This is also true for the chlorine derivative, CCl, as reported by Li and Francisco.[14]

Theoretical studies on iodocarbyne are also scarce, in contrast to existing investigations in the literature on the other halocarbynes. A density functional investigation within the local density approximation augmented by nonlocal exchange corrections for the series of halocarbynes reported results for the equilibrium distance of the ground ($X\ ^2\Pi$) and first excited ($a\ ^4\Sigma^-$) states of CI, as well as the excitation energy, and the bond dissociation energy.[15] Enthalpies of formation of halocarbynes were computed by Marshall *et al*. at the QCISD(T)/6-311+G(3*df*,2*p*) level of theory using optimized geometries at the QCISD(T)/6-311+G(*d*,*p*) level.[16] In a recent study, Bacskay also evaluated the heat of formation of iodocarbyne at a very high level of theory CCSD(T)-CBS with further corrections for core-valence correlation, scalar relativistic, spin-orbit coupling, and thermal effects.[17] First, the atomization energy was computed and then combined with the experimental heats of formation of carbon and iodine through Hess law.

To the best of our knowledge, the energetic profile of the electronic states of iodocarbyne is as yet unknown, in sharp contrast with reported investigations on CF, CCl, and CBr. In this study, in a first step, our major goal is to construct potential energy curves for all states correlating with the two lowest-lying dissociation channels, $C(^3P_g) + I(^2P_u)$ and $C(^1D_g) + I(^2P_u)$ in the Λ + S representation, and then improve upon this description by incorporating spin-orbit effects. In this way, for all bound states, vibrational energies are computed and spectroscopic parameters evaluated; dipole moments functions, and the transition dipole moment function for the $1\ ^4\Sigma^- - X\ ^2\Pi$ transition were also evaluated. It is our hope that the overall characterization of a manifold of electronic states of iodocarbyne and the quantitative data obtained can provide a reliable guide for the experimental spectroscopic investigation of this species.

2. Methods

A direct application of the Wigner-Witmer rules allows us to know the electronic states of a given diatomic system correlating with the pair of atomic fragments.[18] For the case of iodocarbyne, we found out that twelve Λ + S states, namely, $^{2,4}\Sigma^{+}$, $^{2,4}\Sigma^{-}$ (2) , $^{2,4}\Pi$ (2) , and $^{2,4}\Delta$ correlate with the dissociation products C ($^{3}P_g$) + I ($^{2}P_u$), and nine with the second channel, C ($^{1}D_g$) + I ($^{2}P_u$), $^{2}\Sigma^{+}$(2), $^{2}\Sigma^{-}$, $^{2}\Pi$ (3) , $^{2}\Delta$(2), and $^{2}\Phi$. To account for the ground and excited states in a balanced way, we carried out first state averaged complete active space self-consistent (SA-CASSCF) calculations simultaneously for the doublets and quartets by allowing all possible excitations of nine electrons into the active space (3,3,3,0).[19,20] The mixing of spin states at this point is a necessary step since the calculation of spin-orbit matrix elements between states of different multiplicities requires a common set of molecular orbitals. This active space essentially included the valence orbitals of carbon (2*s*, 2*p*), the valence 5*p* orbitals of iodine, and two extra correlating orbitals of symmetries B_1 and B_2. We note that although electron excitations from the molecular orbital associated with orbital 5*s* of iodine were restricted at this stage, these electrons were however correlated in the configuration interaction step described below. Computational code design requires that calculations for a heteronuclear diatomic be done in the C_{2v} point group. In this sub-group of the $C_{\infty v}$ point group, the correspondence between the irreducible representations is: A_1 (Σ^{+}, Δ), B_1 (Π_x) and B_2 (Π_y), and A_2 (Σ^{-}, Δ). In this SA-CASSCF step, a total of 33 states were mixed: A_1 (6), B_1 (6), B_2 (6), A_2 (6) for the doublets and A_1 (2), B_1 (2), B_2 (2) A_2 (3) for the quartets. The configuration state functions generated in this step define the zeroth-order wavefunction for each one of the molecular symmetries. For the doublet states, they have the dimensions of 2212 for A_1 (Σ^{+}, Δ), B_1 and B_2 (Π) symmetries, and 2184 for the A_2 (Σ^{-}, Δ) symmetry; for the quartet states, we obtained 1424 for A_1 (Σ^{+}, Δ), B_1 and B_2 (Π) symmetries, and 1488 for the A_2 (Σ^{-}, Δ) symmetry. As atomic basis for the construction of the molecular orbitals, we employed the augmented correlation consistent polarized valence quintuple-zeta set

(aug-cc-pV5Z) for carbon,[21] and the aug-cc-pV5Z-PP for the iodine atom.[22] The iodine set includes a core (28 electrons) energy consistent relativistic pseudo-potential (PP), namely, ECP28MDF, that is, the 1s-3d core was replaced by an energy consistent pseudo-potential that was optimized in a multiconfigurational Dirac–Hartree–Fock calculation.

The zeroth-order wavefunction constructed in the previous step accounts for static or near degeneracy effects. Now, to incorporate dynamical correlation into the wavefunctions, all single and double electron excitations were next allowed on top of the CASSCF wave functions. Averaged natural orbitals from the CASSCF step were used in the construction of the N-particle space which served as a basis expansion of the final MRCI state function. To make the calculation manageable, use was made of the internally contracted configuration interaction approach (MRCI),[23,24] as implemented in the MOLPRO 2009 suite of programs,[25] which reduced significantly the dimensions of the final wavefunctions. The final space had dimensions of the order of 7.5×10^6 (4.0×10^6) contracted (plus uncontracted single excitations) configurations state functions for the doublets (quartets) depending on the state symmetry and also on the internuclear distance.

Vibrational energies and wavefunctions were computed as solutions of the radial Schrödinger equation for the nuclear motion using the Numerov algorithm as implemented in the LEVEL 8.0 program.[26] The potential energy functions were generated by numerical interpolation of the total energies calculated at 83 internuclear distances, and the spectroscopic constants obtained by standard fitting procedure as described in the literature.[27-29] These energies were corrected by an estimate of the contribution of the missing higher excitations needed to reach the full configuration interaction limit known as the Davidson correction (+Q).[30, 31] With this program, transition probabilities were also computed and used to estimate radiative lifetimes.

Spin-orbit effect calculations were done with a mixed SA-CASSCF/MRCI approach known to give very reliable results in the literature. First, the spin-orbit matrix elements were evaluated

at the CASSCF level with the quintuple-zeta quality basis sets described above in a model space comprising all the 33 states mixed in the SA-CASSCF step Next, the diagonal elements of the spin-orbit matrix were replaced by the highly correlated MRCI+Q energy values of all the Λ + S states. The final Ω energies resulted from the diagonalization of a matrix of the electronic and spin–orbit operators ($H_{el} + H_{SO}$) in the basis of (Λ + S) eigenstates of H_{el}.[32]

3. Results and Discussion

As discussed in Section 2, in the Λ + S representation there are 12 electronic states correlating with the first dissociation channel of CI, $C(^3P_g) + I(^2P_u)$ and nine with the second channel, $C(^1D_g) + I(^2P_u)$; the potential energy curves of these states are depicted in Fig. 1. Complementing this energetic profile, we show in Fig. 2 the potential energy curves of the low-lying relativistic states (Ω) derived from the Λ + S states. In this figure, the energy splittings due to spin-orbit interactions are clearly evident for the states in which it is significant. In Table 1 we present the correlation between the atomic fragments and the relativistic states (Ω), and the energy separations at the dissociation limits predicted in this study and the experimental ones.[33] As expected at this level of calculation, the agreement with the experimental values is very good; for example, the energy difference between the channels $C(^3P_0) + I(^2P_{3/2})$ and $C(^3P_0) + I(^2P_{1/2})$ is predicted to be 7252 cm^{-1}, whereas experimentally it is known to be 7603 cm^{-1}.[33] Also the energy difference between the channels $C(^1D_2) + I(^2P_{3/2})$ and $C(^3P_0) + I(^2P_{3/2})$ amounts to 10 006.6 cm^{-1}, a result also in very good accord with the spectroscopic value of 10 192.6 cm^{-1}.[33] The energy difference between the third and fourth channels, 7252 cm^{-1}, reflects again the energy splitting between $I(^2P_{1/2})$ and $I(^2P_{3/2})$. The spectroscopic parameters associated with the bound (Λ + S) and the Ω states are listed in Table 2.

At the equilibrium distance, the ground state, X $^2\Pi$, with R_e = 3.856 a_0 (2.040 Å) and ω_e = 632 cm^{-1} is dominated by the electronic configuration …$12\sigma^2\ 6\pi^4\ 13\sigma^2\ 7\pi^1$ ($c_0 \sim 0.87$) with a small contribution of …$12\sigma^2\ 6\pi^3\ 13\sigma^2\ 7\pi^2$ ($c_0 \sim 0.15$). In terms of a simple molecular orbital picture, orbitals $6\pi_{x,y}$ are essentially the iodine $5p_{x,y}$ orbitals slightly polarized towards the carbon atom, and $7\pi_{x,y}$ are the carbon $2p_{x,y}$ orbitals; orbital 13σ is a bonding combination between a carbon *sp* hybrid and iodine $5p_z$, and orbital 12σ is associated with the two electrons singlet coupled in carbon. Theoretically, Marshal *et al.*[16] estimated the ground state (X $^2\Pi$) bond length and vibrational parameters of iodocarbyne (CI) at different levels of theory using an effective core potential for iodine (ECP) and also in all electrons calculations (AE). At the MP2(full)/6-31G(*d*), they obtained 3.900 a_0 (2.064 Å) (AE) and 3.872 a_0 (2.049 Å) (ECP) for R_e. With the improved QCISD/6-311G(*d*,*p*) approach the distances increased to 3.923 a_0 (2.076 Å) (AE) and 3.883 a_0 (2.055 Å) (ECP); as for the harmonic frequencies, they obtained 598 (AE) and 602 (ECP) cm^{-1}. At a higher level of theory, QCISD(T)/6-311G3df, 2p), their results were 3.870 a_0 (2.048 Å) (AE) and 3.823 a_0 (2.023 Å) (ECP) for the equilibrium distances, and 627 (AE) and 636 (ECP) cm^{-1} for the harmonic frequencies. As a more realistic value for R_e(CI), they recommended the average of their highest level results, 3.848 a_0 (2.036 Å), as a best estimate of the CI bond length,[16] and 632 cm^{-1} for the harmonic frequency; these values are in very good accord with the more accurate results, 3.856 a_0 (2.040 Å) and 632 $cm^{-1}$of this study. An earlier investigation by Gutsev and Ziegler using density functional theory within the local density approximation augmented by nonlocal exchange corrections (DFT-LDA/NL) obtained 3.831 a_0 (2.027 Å) for the equilibrium internuclear distance of the ground state.[15]

With the inclusion of spin-orbit interactions, the equilibrium distance of the ground state $X_1\ ^2\Pi_{1/2}$ ($\Omega = 1/2$) increased slightly to 3.862 a_0 (2.044 Å), and that of $X_2\ ^2\Pi_{3/2}$ ($\Omega = 3/2$) decreased by just 0.001 a_0, to 3.855 a_0 (2.040 Å); for the harmonic frequencies, the one of the state $X_2\ ^2\Pi_{3/2}$ ($\Omega = 3/2$) remained practically unchanged, 632 cm^{-1}, and that of the state

$^2\Pi_{1/2}$ (Ω = 1/2) decreased by 9 cm^{-1} to 623 cm^{-1}. The excitation energy T_e between the states X_2 $^2\Pi_{3/2}$ (Ω = 3/2) and X_1 $^2\Pi_{1/2}$ (Ω = 1/2) is 833 cm^{-1} (0.103 eV), a relatively small value compared to the energy difference between the multiplets $^2P_{1/2}$ and $^2P_{3/2}$ of iodine, 7603 cm^{-1} (0.876 eV). This magnitude can however be rationalized by noting that the unpaired electron is mostly localized on the carbon atom. In the absence of any experimental data so far for this species, we note that in the case of IO, the best theoretical result reported so far in the literature for the coupling constant (A_e) is −1775 cm^{-1} (ref. [34]), whereas −2091 cm^{-1} was found experimentally;[35] inclusion of core-valence correlation in the spin-orbit calculation improved the IO constant to −1827 cm^{-1}.[34] This difference reflects the expected uncertainty at this level of calculation. For the sake of comparison, in the case of the halocarbynes CCl and CBr, we note that the spin-orbit coupling constant (A_0) has been known to be 135 and 466 cm^{-1}, respectively,[36] whereas for the chalcogen halides, SCl, SBr, and SI, with a π^3 ground state, it follows the sequence −453 [ref. 37], −748 [ref. 38], and −1399 cm^{-1} (ref. 39), respectively.

As to the dissociation energy, without the inclusion of spin-orbit interactions it was estimated to be 23 762 cm^{-1} (67.94 kcal mol^{-1}, 2.946 eV), a value smaller than the one evaluated for CBr, 27 664 cm^{-1} (79.10 kcal mol^{-1}, 3.430 eV).[13] For the relativistic states Ω = 1/2 (I) and Ω = 3/2 (I), we obtained 22 024 cm^{-1} (62.98 kcal mol^{-1}, 2.731 eV) and 21 191 cm^{-1} (60.59 kcal mol^{-1}, 2.627 eV), respectively. Subtracting from these values the zero-point energies, 314 and 306 cm^{-1} for the states 1/2(I), and 3/2(I), respectively, our best estimates for the dissociation energies D_0 are 62.08 and 59.72 kcal mol^{-1}, a result in good agreement with the high level calculation of Bacskay, 61.80 kcal mol^{-1}.[17] These results are also consistent with the DFT-LDA/NL estimate of Gutsev and Ziegler of 61.34 kcal mol^{-1} (2.66 eV) for the dissociation energy.[15]

As an assessment of core-valence correlation effects on the equilibrium distance and harmonic frequency, a spin unrestricted RHF-UCCSD(T)[40-42] geometry optimization with the cc-pwCV5Z[43] and cc-pwCV5Z-PP[44] basis sets for C and I, respectively, was also carried out; in this calculation, the 1*s* electrons of carbon and the 4*s*, 4*p*, and 4*d* of iodine were also included in the excitation process. As verified in our previous study of the SI system, the inclusion of core-valence correlation effects decreases the internuclear distance. In the case of CI, we obtained R_e = 3.823 a_0 (2.023 Å) compared to 3.840 a_0 (2.032 Å) obtained with a correlated calculation of valence electrons only using the same basis sets. For the harmonic frequency, the effect was to increase it from 632 to 639 cm^{-1}.

The first excited quartet in the Λ + S representation, 1 $^4\Sigma^-$, with R_e = 3.836 a_0 (2.030 Å), has an excitation energy (T_e) of 14 136 cm^{-1} (1.753 eV) and is best represented by the configuration …$12\sigma^2\ 6\pi^4\ 13\sigma^1\ 7\pi_x^1\ 7\pi_y^1$ (c_0 ~0.92); this excitation energy is about 11% smaller than that for the corresponding transition in bromocarbyne (CBr), 15 969 cm^{-1}.[13] An energy splitting due to spin-orbit interactions gives rise to the relativistic states Ω = 1/2 (II) (T_e = 14 447 cm^{-1}) and Ω = 3/2 (II) (T_e = 14 585 cm^{-1}), both with R_e = 3.847 a_0 (2.036 Å) and harmonic frequencies of 635 and 638 cm^{-1}, respectively. Note that the equilibrium distances for these states are about 0.02 a_0 shorter and the frequencies 12 and 6 cm^{-1} greater than those of the ground state. In the DFT-LDA/NL calculation of Gutsev and Ziegler,[15] the equilibrium distance of the $^4\Sigma^-$ state turned out to be 3.787 a_0 (2.004 Å), a value shorter by 0.05 a_0 than our more accurate estimate, but consistent with our prediction of a slightly shorter bond length compared with the one of the ground state; their excitation energy of 16 373 cm^{-1} (2.03 eV) overestimates by 16% the more accurate prediction of this study. In the Λ + S representation, the dissociation energy (D_e) of the state $^4\Sigma^-$ is 9662 cm^{-1} (27.63 kcal mol^{-1}, 1.198 eV); inclusion of the zero-

point energy reduces this value to 9360 cm^{-1}(D_0). For the states 1/2(II) and 3/2(II), D_e was estimated to be 7582 and 7447 cm^{-1}, respectively, and 7268 and 7151 $cm^{-1}$for D_0.

As illustrated in Fig. 1, in the Λ + S representation, the states 1 $^4\Pi$ (R_e = 4.782 a_0, T_e = 21 754 cm^{-1}) and 1 $^2\Sigma^+$ (R_e = 4.613 a_0, T_e = 23 029 cm^{-1}) have very shallow wells, whereas the states 2 $^2\Pi$ and 1 $^2\Sigma^-$ are repulsive. A deeper well is exhibited by the state 1 $^2\Delta$ (R_e = 3.806 a_0, T_e = 28 165 cm^{-1}), but an avoided crossing with a higher-lying state gives rise to a hump of 4041 cm^{-1}. It is expected that this state be highly perturbed as it is crossed by the states $^2\Pi$ and $^2\Sigma^-$ between the vibrational states v' = 0, 1, by the state $^2\Sigma^+$ close to v'= 0, and also by the $^4\Pi$ close to the minimum. We also note that in the case of the two states with shallow wells, $^4\Pi$ is crossed by the state $^4\Sigma^-$ close to v' = 1, and $^2\Sigma^+$ is crossed by the repulsive $^2\Pi$ state. With the inclusion of spin-orbit interactions this energetic profile changes significantly, especially in the region above ~30 000 cm^{-1}, where a high density of states and curve crossings are very noticeable. From this picture we can infer that the transitions $^2\Delta$ – X $^2\Pi$, if not strongly perturbed, are very unlikely to occur. The Ω = 5/2 (I) state with a major contribution of $^4\Pi$ at the equilibrium distance has a shallow well with D_e = 1913 cm^{-1}. The percentage composition of the eight lowest-lying Ω states in terms of the Λ + S states for selected distances is summarized in Table 3. A detailed treatment of the interactions in this region with a relatively high density of states is not an easy task and is beyond the present focus of this investigation. Compared to literature studies of other halocarbynes, the overall energetic profiles of the Λ + S electronic states of CI are very similar to the ones reported for CCl and CBr.

A possible route for the spectroscopic characterization of iodocarbyne is to react carbon and iodine atoms in a manner similar to that conducted for the luminescent reaction between Se and F,[45,46] and record the emission spectra due to the spin-orbit forbidden transitions between the

states $X_1\ ^2\Pi_{3/2} - {}^4\Sigma^-_{1/2}$ and $X_1\ ^2\Pi_{3/2} - {}^4\Sigma^-_{3/2}$. These transitions are expected to be Franck-Condon dominant but of low intensity, falling in the spectral region of about 14 500 cm^{-1}.

For the sake of completeness, and of direct comparison with experimental data, we show in Tables 4 and 5 the vibrational spacings $\Delta G_{v+1/2}$, defined as $G(v+1) - G(v)$, and the rotational constants B_v, evaluated as the vibrational average $< v \,|16.8578 / \mu R^2| \, v >$.

The dipole functions for the two lowest-lying bound states are plotted in Fig. 3. The one for the $^2\Pi$ state shows a linear behavior from 3.5 to about 5.0 a_0, changing the polarity close to 4.6 a_0 before reaching a minimum value and then decreasing to zero as the distance increases, as expected for neutral fragments at the dissociation limit; for the state $^4\Sigma^-$, it also shows a linear behavior up to 4.5 a_0. Concerning the polarity of this molecule, the positive value of the dipole moment in this graph indicates the carbon atom as the negative side of the dipole. For the sake of comparison and completeness, we also plotted in the same graph the dipole moment function of the other halocarbynes, CF, CCl, and CBr, and also of CO, all evaluated at the same level of theory used for CI in this work. For the species CO, a classical example, a naïve chemical reasoning would place the negative charge of the dipole on the more electronegative oxygen atom, however, it is known experimentally to have the polarity $C^{\delta-}O^{\delta+}$ [ref. 47], a result also supported by high level calculations.[48,49] As seen in Fig. 3, this is also the case for all the halocarbynes; in this figure, the asterisk symbol indicates the equilibrium distance. Around this distance, the dipole moment function is linear with the polarity $C^{\delta-}X^{\delta+}$and largest for iodocarbyne.

Complementing the description above, we have also evaluated transition probabilities, as expressed by the Einstein emission coefficients ($A_{v'v''}$), Franck-Condon factors, and transition energies $T_{v'v''}$ for the transition 1/2(II) – 1/2(I) (Table 6) and 3/2(II) – 1/2(I) (Table 7). As expected from the positions of the minima of the potential energy curves, the relative intensity predictions based on the Franck-Condon factors are concordant with those evaluated by the

coefficients $A_{v'v''}$. From the transition energies, we can see that transitions between these states are expected to fall in the red region of the visible spectra and are predicted to have very weak intensities. Also from these tables we estimated the radiative lifetime of the state 1/2 (II) (v'= 0) as 140 ms and 714 ms for the state 3/2 (II) (v'= 0). Further spectroscopic information is shown in Table 8 for the dipole moment absorption matrix elements, the average dipole moments, and the Einstein A spontaneous emission coefficients for selected vibrational levels of the state X $^2\Pi_{1/2}$ (1/2(I)).

IV. Conclusion

A manifold of electronic states of iodocarbyne (CI) correlating with the first dissociation channel are reliably characterized for the first time in the literature. Potential energy curves are presented in both the Λ + S and the relativistic Ω representations, and the associated spectroscopic parameters evaluated. In both types of calculations, scalar relativistic effects are accounted for through a pseudopotential for the iodine atom. For the evaluation of spin-orbit effects in the relativistic calculations, all states correlating with the first dissociation channel were taken into account. Dipole moment functions were also evaluated and compared with those of the other carbines CF, CCl, and CBr, and also of CO. These functions clearly show that all these species have a $C^{\delta-}X^{\delta+}$ polarity around the equilibrium distance, the CO molecule being already a classic example; CI has the largest dipole moment among these species. A radiative association between C and I atoms with light emitted in the red region of the visible spectra is suggested as a possible mechanism characterizing the species CI spectroscopically. Transitions probabilities were also evaluated predicting very weak intensities. For the states 1/2(II) and 3/2(II), we have estimated radiative lifetimes of 7.1 and 714 m*s*.

Acknowledgements

T.V.A. expresses his gratitute to Fundação de Amparo à Pesquisa do Estado de São Paulo of Brazil for a post-doctoral fellowship, and F.R.O. acknowledges the academic support of the Conselho Nacional de Desenvolvimento Científico e Tecnológico (CNPq) of Brazil.

References

1 R. A. Moss, M. S. Platz and M. Jones, Jr., *Reactive Intermediate Chemistry*, Wiley-Interscience, Hoboken, NJ, 2004.

2 J. F. Liebman and J. Simons, *Molecular Structure and Energetics*, VCH, Deerfield Beach, Fl., 1986 , Vol. 1.

3 S. H. Kable, S. A. Reid and T. J. Sears, *Int. Rev. Phys. Chem*., 435, **28**, 2009.

4 F. C. James, H. K. J. Choi, B. Ruzicska, O. P. Strausz and T. N. Bell, *The Gas Phase of Carbynes, in Frontiers of Free Radical Chemistry,* Editor, W. A. Pryor, Academic Press, p. 139, 1980.

5 E. O. Fischer, G. Kreis, C. G. Kreiter, J. Muller, G. Huttner and H. Lorenz, *Angew. Chemie*, 564, **12**, 1973.

6 P. J. Brothers and W. R. Roper, *Chem. Rev.*, 1293, **88**, 1988.

7 M. B. Shao, L. Zheng, W. X. Qiao, J. J. Wang and J. H. Wang, *Adv. Synth. Catal.*, 2743, **354**, 2012.

8 X. Wu, *Prog. Chem*., 318, **24**, 2012.

9 B. Ruzsicska, A. Jodhan, H. K. J. Choi, O. P. Strausz and T. N. Bell, *J. Am. Chem. Soc*., 2849, **105**, 1983.

10 K. M. A. Refaey and J. L. Franklin, *Int. J. Mass Spectry & Ion Phys*., 19, **20**, 1976.

11 P. Zou, J. Shu, T. J. Sears, G. E. Hall and S. W. North, *J. Phys. Chem. A*, 1482, **108**, 2004.

12 R. J. Salawitch, *Nature*, 275, **439**, 2006.

13 S. Burrill and F. Grein, *Mol. Phys*., 1891, **105**, 2007.

14 Y. M. Li and J. S. Francisco, *J. Chem. Phys.*, 2192, **114**, 2001.

15 G. L. Gutsev and T. Ziegler, *J. Phys. Chem.*, 7220, **95**, 1991.

16 P. Marshall, A. Misra and M. Schwartz, *J. Chem. Phys.*, 2069, **110**, 1999.

17 G. B. Bacskay, *J. Phys. Chem. A*, 8625, **114**, 2010.

18 G. Herzberg, *Molecular Spectra and Molecular Structure I.: Spectra of Diatomic Molecules,* Van Nostrand Reinhold, New York, 1950.

19 P. J. Knowles and H. -J. Werner, *J. Chem. Phys*., 5053, **82**, 1985.

20 H. -J. Werner and P.J. Knowles, *Chem. Phys. Lett.*, 259, **115**, 1985.

21 R. A. Kendall, T. H. Dunning, Jr. and R. J. Harrison, *J. Chem. Phys*., 6796, **96**, 1992.

22 K. A. Peterson, D. Figgen, E. Goll, H. Stoll and M. Dolg, *J. Chem. Phys.*, 11113, **119**, 2003.

23 P. J. Knowles and H. -J. Werner, *Chem. Phys. Lett.*, 514, **82**, 1988.

24 H. -J. Werner and P. J. Knowles, *J. Chem. Phys.*, 5803, **89**, 1988.

25 H. -J. Werner, P. J. Knowles, R. Lindh, F. R. Manby, M. Schütz, and others *Molpro*, Version 2009.1, A package of Ab Initio Programs, Cardiff University, Cardiff, U.K., 2009. <http://www.molpro.net>.

26 R. J. LeRoy, *LEVEL 8.1 program.* University of Waterloo Chemical Physics Research Report CP-663 (2007). See http://scienide.uwaterloo.ca/~leroy/level.

27 F. R. Ornellas, W. C. Stwalley and W. T. Zemke, *J. Chem. Phys.*, 5311, **79**, 1983.

28 F. B. C. Machado and F. R. Ornellas, *J. Chem. Phys.*, 7237, **94**, 1991.

29 A. C. Borin and F. R. Ornellas, *J. Chem. Phys.*, 8761, **98**, 1993.

30 E. R. Davidson and D. W. Silver, *Chem. Phys. Lett*., 403, **52**, 1977.

31 H. -J. Werner, M. Kállay and J. Gauss, *J. Chem. Phys.*, 034305, **128**, 2008.

32 A. Berning, M. Schweizer, H. -J. Werner, P. J. Knowles and P. Palmieri, *Mol. Phys*., 1283, **98**, 2000.

33 A. A. Radzig and B. M. Smirnov, *Reference Data on Atoms, Molecules, and Ions*, Springer-Verlag, Berlin, 1985.

34 K. A. Peterson, B. C. Shepler, D. Figgen and H. Stoll, *J. Phys. Chem. A*, 13877, **110**, 2006.

35 M. K. Gilles, M. L Polak and W. C. Lineberger, *J. Chem. Phys.*, 4723, **95**, 1991.

36 K. -P. Huber and G. Herzberg, *Molecular Structure and Molecular Spectra. IV Constants of Diatomic Molecules*, Van Nostrand Reinhold, New York, 1979.

37 F. B. C. Machado, S. M. Resende and F. R. Ornellas, *Mol. Phys*., 699, **100**, 2001.

38 F. R. Ornellas, *J. Chem. Phys*., 114314, **125**, 2006.

39 A. G. S. de Oliveira-Filho and F. R. Ornellas, *Chem. Phys. Lett*., 31, **510**, 2011.

40 J. D. Watts, J. Gauss and R. J. Bartlett, *J. Chem. Phys*., 8718, **98**, 1993.

41 P. J. Knowles, C. Hampel and H. -J. Werner, *J. Chem. Phys.*, 5219, **99**, 1993.

42 P. J. Knowles, C. Hampel and H. -J. Werner, *J. Chem. Phys*., 3106, **112**, 2000.

43 K. A. Peterson and T. H. Dunning, Jr., *J. Chem. Phys.*, 10548, **117**, 2002.

44 K. A. Peterson and K. E. Yousaf, *J. Chem. Phys*., 174116, **133**, 2010.

45 W. Hermoso and F. R. Ornellas, *J. Chem. Phys*., 194316, **132**, 2010.

46 W. G. Thorpe, W. R. Carper and S. J. Davis, *J. Chem. Phys.*, 4544, **83**, 1985.

47 B. Rosenblum, A. H. Nethercot, Jr. and C. H. Townes, *Phys. Rev.*, 400, **109**, 1958.

48 D. Feller, C. M. Boyle and E. R. Davidson, *J. Chem. Phys.*, 3224, **86**, 1987.

49 G. E. Scuseria, M. D. Miller, F. Jansen and J. Geertsen, *J. Chem. Phys.*, 6660, **94**, 1991.

Table 1. Low-lying electronic states of the molecule CI, their dissociation channels, and energy separation at dissociation limit including spin-orbit effects.

Atomic fragments	Molecular States (Ω)	ΔE / cm^{-1}	
		Exp.[a]	Theor.
$C(^3P_0) + I(^2P_{3/2})$	3/2, 1/2	0.0	0.0
$C(^3P_1) + I(^2P_{3/2})$	5/2, 3/2, 3/2, 1/2, 1/2, 1/2	16.4	13.7
$C(^3P_2) + I(^2P_{3/2})$	7/2, 5/2, 5/2, 3/2, 3/2, 3/2, 1/2, 1/2, 1/2, 1/2	43.4	36.3
$C(^3P_0) + I(^2P_{1/2})$	1/2	7 603.1	7 252.2
$C(^3P_1) + I(^2P_{1/2})$	3/2, 1/2, 1/2	7 619.5	7 257.2
$C(^3P_2) + I(^2P_{1/2})$	5/2, 3/2, 3/2, 1/2, 1/2	7 646.6	7 265.2
$C(^1D_2) + I(^2P_{3/2})$	7/2, 5/2, 5/2, 3/2, 3/2, 3/2, 1/2, 1/2, 1/2, 1/2	10 192.6	10 006.6
$C(^1D_2) + I(^2P_{1/2})$	5/2, 3/2, 3/2, 1/2, 1/2	17 795.7	17 258.4

[a] Ref. [33]

Table 2. Excitation energy (T_e) in cm^{-1}, equilibrium distance (R_e) in a_0, dissociation energy (D_e) in kcal/mol, and vibrational and rotational constants, all in cm^{-1}, of the Λ + S and Ω states of the species CI.

Λ + S states	T_e	R_e	D_e	ω_e	$\omega_e x_e$	$\omega_e y_e$	B_e	$10^{-2}\ \alpha_e$
$X\ ^2\Pi$	0	3.856	23 762	631.8(20)	3.423	–0.003	0.3694	0.281
$1\ ^4\Sigma^-$	14 136	3.836	9 662	610.9(20)	4.387	–0.194	0.3719	0.237
$1\ ^4\Pi$	21 754	4.782	2 046	214.3(5)	5.967	–0.052	0.2415	0.548
$1\ ^2\Sigma^+$	23 029	4.613	731	246.5(4)	–5.652	–2.014	0.2566	0.221
$1\ ^2\Delta$	28 165	3.806	–4 404	567.8(4)	13.682	–0.731	0.3789	0.526

Ω states	T_e	R_e	D_e	ω_e	$\omega_e x_e$	$\omega_e y_e$	B_e	$10^{-2}\ \alpha_e$
1/2(I)	0	3.862	22 024	622.9(20)	3.507	–0.004	0.3675	0.285
3/2(I)	833	3.855	21 191	632.3(20)	3.452	–0.005	0.3692	0.279
1/2(II)	14 447	3.847	7 582	634.8(20)	4.091	–0.005	0.3735	0.385
3/2(II)	14 585	3.847	7 447	637.6(20)	4.128	–0.009	0.3729	0.348
5/2(I)	20 050	4.781	1 911	214.4(5)	6.715	–0.715	0.2412	0.573
3/2(III)	21 098	4.828	985	187.8(2)	15.252	–2.059	0.2361	0.693
1/2(VI)	26 473	4.579	–6 708					
3/2(IV)	29510	4.000	–7 508					

Table 3. Composition (in %) of the lowest-lying Ω states of CI molecule at various internuclear distances.

State	R (a_0)	$X\,^2\Pi$	$1\,^4\Sigma^-$	$1\,^4\Pi$	$1\,^2\Sigma^+$	$2^2\Pi$	$1\,^2\Sigma^-$	$1\,^2\Delta$
1/2(I)	3.2	99.6						
	3.8	98.7						
	4.4	98.8						
	6.0	89.1						
3/2(I)	3.2	99.5						
	3.8	99.2						
	4.4	97.2						
	6.0	87.5						
1/2(II)	3.2		99.1					
	3.8		98.1					
	4.4		90.1	9.2				
	6.0			99,5				
3/2(II)	3.2		99.4					
	3.8		98.3					
	4.4		90.8	6.7				
	6.0		10.9	76.1				
5/2(I)	3.2		37.4					61.2
	3.8			99.9				
	4.4			99.9				
	6.0		32.6	52.2		11.6		
3/2(III)	3.2		39.9					61.9
	3.8			75.5	12.4	10.5		
	4.4			76.1		17.8		
	6.0		28.5	10.8		52.6		
1/2(VI)	3.2			93.2				
	3.8			6.7		5.6		84.3
	4.4		7.3	49.1		39.8		
	6.0		35.6	56.0				
3/2(IV)	3.2			98.2				
	3.8			54.9		25.8		12.1
	4.4			25.3		6.6	65.9	
	6.0					16.6	60.0	18.1

Table 4. Vibrational spacing $\Delta G_{v+1/2}$ (in cm^{-1}) and zero point energies (E_0) for selected electronic states of CI.

	Λ + S states					Ω states					
v	X $^2\Pi$	1 $^4\Sigma^-$	1 $^4\Pi$	1 $^2\Sigma^+$	1 $^2\Delta$	1/2(I)	3/2(I)	1/2(II)	3/2(II)	5/2(I)	3/2(III)
0	624	606	202	251	577	624	615	579	583	201	164
1	618	593	190	244	555	619	609	563	567	188	152
2	611	579	177	226	532	612	602	545	549	176	
3	604	564	163	195	507	605	594	526	530	162	
4	597	549	151			597	587	506	509	151	
5	591	534				591	580	484	487		
6	584	519				584	574	460	463		
7	577	504				577	567	434	434		
8	570	486				569	559	404	401		
9	563	467				561	552	371	363		
10	556	445				554	544	336	321		
E_0	314	302	103	277	294	314	306	295	296	103	92

Table 5. Rotational constants B_v (in cm^{-1}) and zero point energies (E_0) for selected electronic states of CI.

v	X $^2\Pi$	1/2(I)	3/2(I)	1 $^4\Sigma^-$	1/2(II)	3/2(II)
0	0.3681	0.3679	0.3662	0.3722	0.3689	0.3694
1	0.3652	0.3650	0.3632	0.3683	0.3645	0.3650
2	0.3623	0.3621	0.3603	0.3643	0.3599	0.3604
3	0.3595	0.3592	0.3574	0.3604	0.3550	0.3556
4	0.3567	0.3564	0.3546	0.3563	0.3499	0.3505
5	0.3538	0.3535	0.3517	0.3520	0.3443	0.3450
6	0.3510	0.3506	0.3488	0.3473	0.3381	0.3387
7	0.3481	0.3477	0.3458	0.3422	0.3309	0.3314
8	0.3453	0.3449	0.3430	0.3367	0.3227	0.3227
9	0.3424	0.3421	0.3400	0.3308	0.3132	0.3124
10	0.3394	0.3392	0.3370	0.3245	0.3027	0.3004

	1 $^4\Pi$	5/2(I)	3/2(III)	1 $^2\Sigma^+$	1 $^2\Delta$
0	0.2385	0.2380	0.2322	0.2553	0.3762
1	0.2328	0.2322	0.2220	0.2510	0.3700
2	0.2255	0.2249	0.2028	0.2458	0.3634
3	0.2179	0.2173		0.2380	0.3553
4	0.2101	0.2096		0.2198	0.3470
5	0.1936	0.2021			

Table 6. Einstein emission $A_{v'v''}$ (in s^{-1}) coefficients, and Franck-Condon factors (in parentheses), and transition energies $T_{v'v''}$ (cm^{-1}, in italics) for the transition 1/2(II) - 1/2(I) of the CI molecule.

v''	$v' = 0$	$v' = 1$	$v' = 2$	$v' = 3$	$v' = 4$	$v' = 5$	$v' = 6$
0	**133.99**	0.60	0.01	0.03	0.16	0.17	0.03
	(0.994)	(0.005)	(0.000)	(0.000)	(0.000)	(0.000)	(0.000)
	14 436	*15 014*	*15 577*	*16 123*	*16 649*	*17 155*	*17 639*
1	5.24	**130.45**	2.95	0.23	0.48	0.42	0.22
	(0.005)	(0.987)	(0.005)	(0.003)	(0.000)	(0.000)	(0.000)
	13 820	*14 399*	*14 962*	*15 508*	*16 034*	*16 539*	*17 023*
2	0.59	9.90	**143.06**	9.87	1.04	1.16	0.79
	(0.001)	(0.004)	(0.986)	(0.002)	(0.000)	(0.000)	(0.000)
	13 211	*13 790*	*14 535*	*14 899*	*15 425*	*15 930*	*16 141*
3	0.13	3.26	15.71	**155.23**	21.99	2.55	1.67
	(0.000)	(0.003)	(0.001)	(0.982)	(0.007)	(0.012)	(0.000)
	12 609	*13 188*	*13 751*	*14 297*	*14 823*	*15 328*	*15 812*
4	0.15	1.03	7.32	20.47	**163.21**	38.60	4.49
	(0.000)	(0.000)	(0.006)	(0.000)	(0.963)	(0.011)	(0.016)
	12 015	*12 594*	*13 157*	*13 702*	*14 228*	*14 734*	*15 218*
5	0.10	0.48	2.43	11.95	22.29	**160.07**	58.56
	(0.000)	(0.000)	(0.000)	(0.013)	(0.006)	(0.909)	(0.050)
	11 428	*12 007*	*12 570*	*13 115*	*13 641*	*14 147*	*14 631*
6	0.02	0.20	0.95	3.68	15.45	21.40	**147.5**
	(0.000)	(0.000)	(0.000)	(0.000)	(0.023)	(0.025)	(0.800)
	10 847	*11 426*	*11 989*	*12 535*	*13 061*	*13 567*	*14 051*

Table 7. Einstein emission $A_{v'v''}$ (in s^{-1}) coefficients, and Frank-Condon factors (in parentheses), and transition energies $T_{v'v''}$ (cm^{-1}, in italics) for the transition 3/2(II) - 1/2(I) of the CI molecule.

v''	$v' = 0$	$v' = 1$	$v' = 2$	$v' = 3$	$v' = 4$
0	**0.96**	0.14	0.11	0.00	0.10
	(0.992)	(0.007)	(0.000)	(0.000)	(0.000)
	14 575	*15 157*	*15 724*	*16 273*	*16 803*
1	0.24	**1.82**	0.17	0.00	0.02
	(0.006)	(0.982)	(0.008)	(0.003)	(0.000)
	13 960	*14 542*	*15 109*	*15 685*	*16 188*
2	0.16	0.33	**0.94**	0.16	0.00
	(0.001)	(0.007)	(0.981)	(0.004)	(0.006)
	13 351	*13 933*	*14 500*	*15 049*	*15 579*
3	0.01	0.01	0.27	**0.75**	0.08
	(0.000)	(0.000)	(0.004)	(0.981)	(0.000)
	12 749	*13 331*	*13 898*	*14 447*	*14 977*
4	0.03	0.00	0.01	0.15	**0.73**
	(0.000)	(0.000)	(0.007)	(0.012)	(0.969)
	12 154	*12 737*	*13 303*	*13 852*	*14 382*

Table 8. Dipole moment absorption matrix elements $\mu_{v',1;v'',1}$ in upper right and average dipole moment on the diagonal, both in a.u.. In the lower left, Einstein A spontaneous emission coefficients $A_{v',1;v'',1}$ (in s^{-1}) for the $X\ ^2\Pi_{1/2} - X\ ^2\Pi_{1/2}$ bands of CI.

$v' \setminus v''$	0	1	2	3	4	5
0	**0.6425**	–0.0866	0.0048	–0.0001	0.0000	0.0000
1	13.2063	**0.6221**	–0.1221	0.0084	–0.0003	0.0000
2	0.3174	25.4801	**0.6018**	–0.1492	0.0121	–0.0005
3	0.0010	0.9514	36.7566	**0.5818**	–0.1718	0.0159
4	0.0001	0.0035	1.9003	47.0597	**0.5620**	–0.1914
5	0.0000	0.0003	0.0087	3.1638	56.4612	**0.5421**

Figure Captions

Fig. 1. Potential energy curves of the lowest-lying Λ + S doublets and quartets states of the molecule CI.

Fig. 2. Potential energy curves for the some of the lowest-lying doublets and quartets Ω states of the molecule CI.

Fig. 3. Dipole moment functions $\mu(R)$, in atomic units, for the states X $^2\Pi$ and a $^4\Sigma^-$of the molecule CI, and for the ground state of the species CF, CCl, CBr, and CO. The value of the moment at the equilibrium distance is marked by the symbol *.